Solid State Phenomena
ISSN: 1662-9779, Vol. 390, pp 163-172
doi:10.4028/p-cNIr4V

Submitted: 2026-01-19
Revised: 2026-02-16
Accepted: 2026-02-21
Online: 2026-04-17

Study on the Effects of Grain Shape, Size and Size Distribution on the Mechanical Behavior of Metals

BOCAN Ruxandra[1,2,a*], PERDAHCIOGLU Semih [1,b], and VAN DEN BOOGAARD Ton[1,c]

[1]Chair of Nonlinear Solid Mechanics, University of Twente, Enschede, The Netherlands,
[2]M2i, Materials Innovation Institute
[a]ruxandra.bocan@utwente.nl, [b]e.s.perdahcioglu@utwente.nl ,
[c]a.h.vandenboogaard@utwente.nl

Keywords: Crystal Plasticity, Gradient Enhanced Crystal Plasticity, Grain Size Distribution, Grain Aspect Ratio

Abstract. Crystal plasticity finite element (CPFE) simulations of three-dimensional representative volume elements (RVEs) enable the prediction of polycrystalline material behavior under complex loading conditions. Plastic deformation is modeled through crystallographic slip on lattice slip systems, subject to the Schmid yield criterion based on the maximum resolved shear stress (CRSS). In this work, an efficient rate-independent crystal plasticity (CP) and gradient enhanced crystal plasticity (GECP) formulation is used to investigate the influence of microstructural characteristics on the mechanical performance of FCC materials. Three-dimensional periodic RVEs with irregular grain morphologies are simulated within Abaqus/Standard to study the effects of grain size, grain size distribution, and grain shape under uniaxial loading. Comparative analyses between the CP and GECP frameworks are performed to assess the predictive capabilities and applicability for increasingly heterogeneous microstructures. The results demonstrate that GECP accurately captures grain size dependent work hardening and grain size distribution effects through the intrinsic length scale introduced by strain gradient calculations. In contrast, grain shape variations result in only minor changes in the macroscopic response for both frameworks.

Introduction

Constitutive micromechanical models based on Crystal Plasticity have become increasingly used to predict material performance under complex loading conditions and manufacturing processes. With advances in computational efficiency, such finite element models also aid in gaining a more fundamental understanding of the effects microstructural parameters have on the overall macroscopic behavior. As a result, crystal plasticity formulations are particularly suited for studying the deformation of heterogeneous structures with physically accurate material descriptions.

Within the crystal plasticity framework, plastic deformation occurs through dislocation movement along slip planes of the crystallographic lattice. The evolution of plastic flow is governed by the assumption that slip is allowed only on slip systems for which the resolved shear stress (RSS) reaches the critical resolved shear stress (CRSS) [1]. Hardening models have been developed that relate this critical lattice resistance to the accumulation of immobile dislocations. Two dislocation types can be distinguished, namely statistically stored dislocations (SSDs) and geometrically necessary dislocations (GNDs) [2]. GNDs arise from strain incompatibilities between neighboring grains undergoing non-uniform plastic deformation and are associated with regions of high plastic strain gradients [3]. Their generation is introduced as an additional hardening mechanism into the crystal plasticity framework, which is directly linked to an intrinsic material length scale, responsible for size-dependent strengthening effects [4]. Frameworks that incorporate this additional hardening mechanism through strain gradient computations are referred to as gradient enhanced crystal plasticity formulations.

There is relatively limited research on the relation between granular microstructural parameters, such as grain size and shape, and the resulting macroscopic mechanical response. Although phenomena such as grain size dependent hardening, described by the Hall-Petch relation, are widely accepted

within the metal industry, many numerical studies remain restricted to two dimensional simulations. Recent developments in rate-independent crystal plasticity formulations allow for the simulation of realistic, three-dimensional RVEs within feasible computation times [5]. In addition, advances in numerical implementation and solution strategies, such as the stress update procedure in [6] allow for the efficient computation in the three-dimensional domain.

The incorporation of dislocation density based hardening without the introduction of additional length scale parameters was first proposed in [7]. Subsequent work extended this approach by including plastic strain gradient calculation into the evolution of GND densities with flow stress [8]. Together, these developments make it possible to efficiently conduct simulations of realistic three-dimensional structures that account for grain size effects using physically motivated descriptions.

This work aims to improve the understanding of the influence of microstructural features on the mechanical performance of metals through crystal plasticity simulations of realistic three-dimensional polycrystalline structures using the described algorithmic frameworks. A quantitative comparative study between conventional CP and GECP is conducted to establish relations between polycrystalline grain parameters and observed material response. The applicability and accuracy of the current rate-independent frameworks are investigated for uniaxial loading conditions of isotropic materials.

Crystal Plasticity Constitutive Framework

In this section a short description of the crystal plasticity and gradient enhanced crystal plasticity formulations is given. Plastic deformation is assumed to occur through dislocation motion along the slip systems of the crystallographic lattice. The constitutive formulation used in this work is based on continuum mechanics kinematics, a flow rule based on Schmid slip system activation, and a rate independent hardening law formulated in terms of the total dislocation density and slip system resistance evolution. Both conventional Crystal Plasticity (CP) and Gradient Enhanced Crystal Plasticity (GECP) formulations are considered. For a more detailed description of the theoretical formulations and tensor decompositions, the reader is referred to [5].

At the core of the CP formulation lies the multiplicative decomposition of the deformation gradient $\mathbf{F}$ into elastic $\mathbf{F}^{\mathrm{e}}$ and plastic parts $\mathbf{F}^{\mathrm{p}}$,

$$\mathbf{F} = \hat{\mathbf{F}}^{\mathrm{e}}\,\mathbf{F}^{\mathrm{p}} \tag{1}$$

where $\mathbf{F}^{\mathrm{p}}$ accounts for permanent deformation due to shearing of the crystallographic lattice. Plastic deformation is assumed to occur solely due to dislocation slip on specific slip systems and is assumed to leave the structure in a stress-free, undistorted intermediate configuration. The elastic part $\mathbf{F}^{\mathrm{e}}$ accounts for the change in stress through elastic distortion and rigid body rotation, mapping the intermediate configuration to the current one. The ($\hat{}$) notation is used to denote variables pushed from the intermediate configuration to the current one, while the remaining variables are defined conventionally. The corresponding velocity gradient $\mathbf{L}$ can be further decomposed into plastic and elastic contributions, $\mathbf{L} = \hat{\mathbf{L}}^{\mathrm{e}} + \hat{\mathbf{L}}^{\mathrm{p}}$. The plastic part of velocity gradient describes the rate at which the crystallographic lattice plastically distorts and is expressed as a sum of plastic slip rates $\dot{\gamma}^{(\alpha)}$ over all active slip systems:

$$\hat{\mathbf{L}}^{\mathrm{p}} = \sum_{\alpha=1}^{n} \dot{\gamma}^{(\alpha)} \left(\hat{\mathbf{s}}^{(\alpha)} \otimes \hat{\mathbf{n}}^{(\alpha)} \right) \tag{2}$$

where the slip systems α, with slip direction $\hat{\mathbf{s}}^{(\alpha)}$ and slip plane normal $\hat{\mathbf{n}}^{(\alpha)}$, are defined in the current configuration. The total plastic deformation of a crystal is obtained through superposition of shear distortions on all active slip systems.

The formulation of rate-independent CP follows Schmid's law, stating that slip occurs only when the resolved shear stress, $\tau^{(\alpha)}$ (RSS), on slip system α, exceeds the slip resistance $\tau^{\mathrm{c}(\alpha)}$, also referred to as the critical resolved shear stress (CRSS):

$$\phi^{(\alpha)}(\boldsymbol{\sigma}, \boldsymbol{\gamma}) = \tau^{(\alpha)}(\boldsymbol{\sigma}) - \tau^{\mathrm{c}(\alpha)}(\boldsymbol{\gamma}) \leq 0 \tag{3}$$

where the above mentioned equation represents the yield function for each system within the polycrystal, and $\boldsymbol{\gamma}$ denotes the vector of accumulated slip over all slip systems.

The total stress of the material is defined using the generalized Hooke's law, with only the elastic part contributing to the stress:

$$\overset{\circ}{\boldsymbol{\sigma}} = \hat{\mathbb{C}}^{\mathrm{e}} : \hat{\mathbf{D}}^{\mathrm{e}} \tag{4}$$

where $\hat{\mathbb{C}}^{\mathrm{e}}$ the elasticity tensor of the lattice and $\overset{\circ}{\boldsymbol{\sigma}}$ denotes the objective rate of the Cauchy stress, capable of allowing for large rotations. The resolved shear stress is then obtained by projecting the stress onto the slip system shear direction:

$$\tau^{(\alpha)} = \boldsymbol{\sigma} : \hat{\mathbf{P}}^{(\alpha)} = \boldsymbol{\sigma} : \frac{1}{2}\left[\hat{\mathbf{s}}^{(\alpha)} \otimes \hat{\mathbf{n}}^{(\alpha)} + \hat{\mathbf{n}}^{(\alpha)} \otimes \hat{\mathbf{s}}^{(\alpha)}\right] \tag{5}$$

where $\hat{\mathbf{P}}^{(\alpha)}$ is the symmetric Schmid tensor.

Hardening in crystal plasticity is a result of the increase in slip resistance with the accumulation of dislocations. The relation between shear flow stress and dislocation density is given by a Taylor-type hardening law, where the CRSS on each slip system is expressed as:

$$\tau^{\mathrm{c}(\alpha)} = \tau_0 + Gb\sqrt{\sum_{\beta=1}^{n} Q^{(\alpha\beta)}\,\rho^{(\beta)}} \tag{6}$$

where τ_0 is the base resistance to slip due to lattice friction [9], G is the shear modulus, b is the Burgers vector length, and $Q^{(\alpha\beta)}$ is the latent hardening matrix, accounting for interactions between slip systems. In [10] it is shown that there can be up to six independent variables within this matrix (Q_0 to Q_5) for a Face-Centered Cubic (FCC) lattice. The superscript β represents all possible slip systems within one crystal of the lattice. The total dislocation density $\rho^{(\beta)}$ consists of contributions from both statistically stored dislocations (SSDs) and geometrically necessary dislocations (GNDs), with the latter included only in the gradient enhanced formulation.

For the two dislocation types, the evolution of dislocation densities within the same crystal is connected to the amount of accumulated plastic slip. For SSDs, a phenomenological formulation [11] is implemented, in which the SSD density, $\rho_{\mathrm{SSD}}^{(\alpha)}$, increases with accumulated slip and approaches a saturation value $\rho_{\mathrm{SSD}}^{\infty}$:

$$\rho_{\mathrm{SSD}}^{(\alpha)} = \rho_{\mathrm{SSD}}^{\infty}\left[1 - \left(1 - \frac{\rho_{\mathrm{SSD}}^{0}}{\rho_{\mathrm{SSD}}^{\infty}}\right)\exp\left(-\frac{\gamma^{(\alpha)}}{\gamma_{\infty}}\right)\right] \tag{7}$$

where ρ_{SSD}^{0} is the initial density and γ^{∞} is the saturation slip.

Moreover, within GECP, GNDs are introduced to maintain compatibility associated with non-uniform plastic deformation between polycrystalline grains. GNDs are related to the gradients of plastic slip through the Burgers tensor. By projecting the gradients of slip $\nabla\gamma^{(\alpha)}$ onto the slip direction and dislocation line direction, edge and screw GND densities are obtained:

$$\rho_{\mathrm{GND,e}}^{(\alpha)} = -\mathbf{s}^{(\alpha)} \cdot \nabla\gamma^{(\alpha)} \tag{8}$$

$$\rho_{\mathrm{GND,s}}^{(\alpha)} = \mathbf{l}^{(\alpha)} \cdot \nabla\gamma^{(\alpha)} \tag{9}$$

GND densities introduce an intrinsic material length scale into the formulation through their direct dependence on strain gradients. The resulting hardening law leads to an enhanced formulation capable of capturing size-dependent mechanical behavior, such as grain size and shape effects in polycrystalline materials.

To solve the constitutive equations of the rate-independent CP and GECP formulations, an implicit stress-update algorithm is used. The evolution of stress during deformation is governed by the enforcement of the Schmid yield and the associated Kuhn Tucker conditions at the end of each increment, ensuring that plastic flow occurs only on active slip systems. The algorithm is based on the Successive One-Dimensional Solution Steps (SODS) method, which determines slip increments without requiring an active set search. For a more detailed explanation of the numerical implementation and solution procedure, the reader is referred to [6].

Numerical Framework and RVE Construction

The two frameworks have been implemented into Finite Element (FE) formulations using a computational homogenization approach. Numerical simulations are performed on three-dimensional finite element representative volume elements (RVEs) to model the polycrystalline microstructure. Regular and irregularly shaped periodic RVEs are generated using the Voro++ software library [12] and meshed within GMSH [13]. The microstructures obtained present statistically representative grain morphologies with control of grain size, size distribution, and aspect ratio. Periodic boundary conditions are applied to the model to ensure consistency and kinematic compatibility with the macroscopic scale. The algorithms used are implemented through FORTRAN modules as independent Abaqus material subroutines. The algorithm consists of a fully implicit stress and strain update scheme implemented within the Abaqus UMAT subroutine. For the Gradient Enhanced formulation, the scheme is weakly coupled with an explicit subroutine, UExternalDB, which solves for the gradients of plastic slip and updates the corresponding shear stresses at the following iterative steps. All simulations are conducted under identical uniaxial loading conditions up to 20% strain to allow for a consistent comparison background. The work is carried out for isotropic FCC materials.

The proper selection of an RVE is essential to ensure that the numerical response is independent of the specific microstructural composition and is statistically representative of the macroscopic behavior of the material. A systematic study was conducted to assess convergence with respect to the number of grains and mesh discretization for the homogenized response of RVEs with uniform grain size and distribution. The validated RVEs yield stable and isotropic responses with good computational efficiency. Subsequently, these RVEs are used to study morphological variations, ensuring a reliable comparison of grain size and grain shape effects. A detailed description of the RVE determination procedure is provided in [14].

Results

In this section, the numerical results obtained from three-dimensional RVE simulations are presented and discussed, focusing on the influence of grain size, grain size distribution, and grain morphology on the macroscopic response under uniaxial loading up to 20% strain along the principal displacement directions. The predictive capabilities of conventional crystal plasticity (CP) and gradient enhanced crystal plasticity (GECP) are systematically compared.

RVE isotropy and framework validation

Prior to investigating microstructural effects, the isotropy and representativeness of the selected RVEs are evaluated for both CP and GECP frameworks. The RVEs used in this study, illustrated in Fig. 1, are generated such that the geometrical grain arrangement is varied, with different degrees of uniformity in grain positioning and shape, while variations in crystallographic grain orientations are also considered. In the present work, only the behavior of the irregular RVE is described.

For RVEs with uniform grain size distribution and morphology, both frameworks provide stable and consistent macroscopic stress-strain responses with limited directional differences. The small variations observed, within an error range of $1-2\%$, between stresses in the principal loading directions are mainly attributed to differences in the assigned grain orientation sets, while changes in geometrical

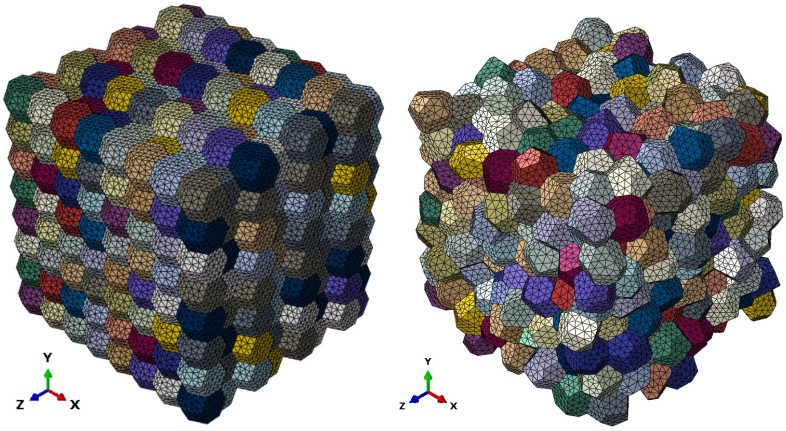

(a) *Regular RVE* (b) *Irregular RVE*

Fig. 1: *3D periodic RVEs with uniform grain size distribution and different degrees of geometrical regularity: (a) regular RVE and (b) irregular RVE. The structures differ in grain positioning and grain shape uniformity. Both consist of 512 grains and approximately 250,000 finite elements, used to assess isotropy and material representativeness*

arrangement result in smaller variations. The isotropic error is further observed to decrease with increasing regularity of the microstructural arrangement. The inclusion of strain-gradient contributions into the GECP framework does not change the sensitivity to microstructural variations, with both the overall behavior and the isotropic response preserved. These results confirm that the selected RVEs provide a suitable basis for modeling isotropic materials within rate-independent crystal plasticity formulations. The RVEs further provide a reliable basis for comparison in subsequent investigations of grain size, grain size distribution and grain shape effects.

Influence of grain size on work hardening behavior (GECP framework)

The influence of grain size on the macroscopic response is examined through the intrinsic length scale introduced in the GECP framework. The simulations predict an increase in flow stress with decreasing gain size, consistent with strengthening concepts such as the Hall-Petch effect, for identical RVE geometries and assigned crystallographic orientation sets as used in the CP simulations. While no shift in the yield stress is observed due to the absence of an initialization relation between grain size and dislocation density in the algorithm, grain refinement manifests through enhanced work hardening. Reducing the grain size from 77 to 9 results in an approximate $14-15\%$ increase in stress, as shown in Fig. 2. This behavior is associated with higher plastic strain gradients and the resulting accumulation of geometrically necessary dislocations (GNDs) at grain boundaries, as confirmed by spatial distribution of GND density, Fig. 5a. Furthermore, finer-grained RVEs also exhibit increased mechanical stability, Fig. 3, as assessed using Considere's criterion, reflected by a shift of the necking point to higher strains and stresses in the absence of explicit damage and localization mechanisms.

In contrast, the classical CP formulation does not capture size dependent work hardening behavior, with no systematic change in response with varying RVE volumes. These results demonstrate that the constitutive inclusion of strain gradients in the hardening law is essential for capturing physically meaningful grain size effects for polycrystalline materials.

Influence of grain size distribution

To further investigate microstructural heterogeneity, RVEs with varying grain size distributions and identical crystallographic orientations are analyzed. The grain size distribution is varied under constant RVE volume constraints, resulting in the presence of larger grains and considerably smaller ones with increasing degrees of heterogeneity, as shown in Fig. 4. The grain size variation is measured using a coefficient of variation parameter, defined as c.o.v$= s/r_{\text{mean}}$, where s is the standard deviation of grain radius and r_{mean} is the mean grain radius. For small coefficients of variations (c.o.v of 0.1), both

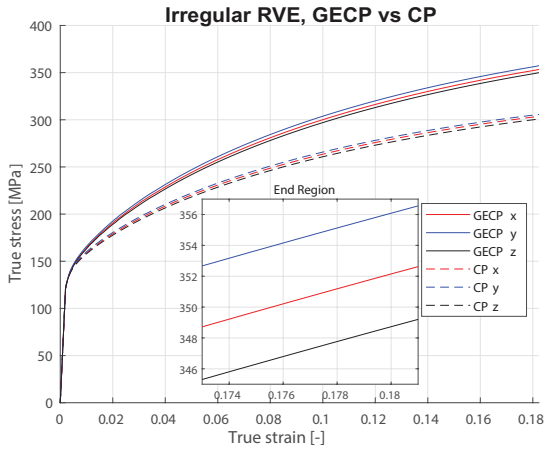

Fig. 2: *Macroscopic true stress-strain response from Abaqus implicit simulations for the irregular RVE under uniaxial loading up to* 20% *strain. Results are shown for both CP(- -) and GECP (–) along the principal loading directions. GECP formulation predicts increased hardening for an average uniform grain size of* 9.

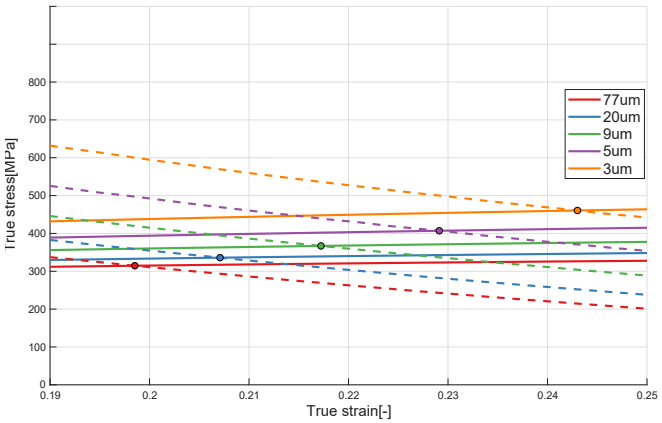

Fig. 3: *Intersection of the true stress-strain (-) and stiffness curves (- -) for RVEs with decreasing grain size. Mechanical stability limit based on the Considere's criterion of necking: onset of reduced resistance to further plastic deformation*

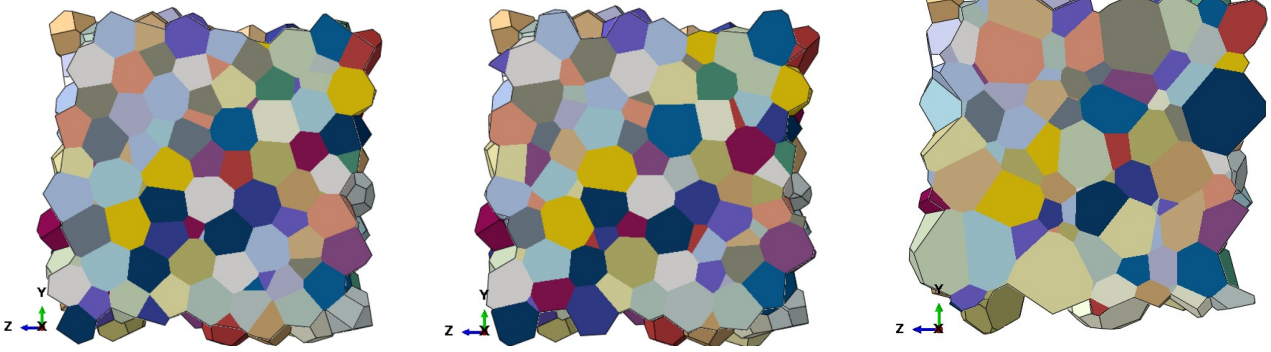

(a) *Uniform grain size, c.o.v=0.0*

(b) *Grain size distribution, c.o.v=0.1*

(c) *Grain size distribution, c.o.v=0.3*

Fig. 4: *Grain size distribution in periodic RVEs: Geometry plane cut (x-y) for 3D periodic irregular RVE with increasing grain size distribution under constant RVE volume constraints. (a) Base geometry with uniform grain size, (b) coefficient of variation c.o.v=0.1, with proportional increase and decrease in individual grain volumes, (c) c.o.v=0.3 with dominant large grains surrounded by smaller grains to preserve the overall RVE volume*

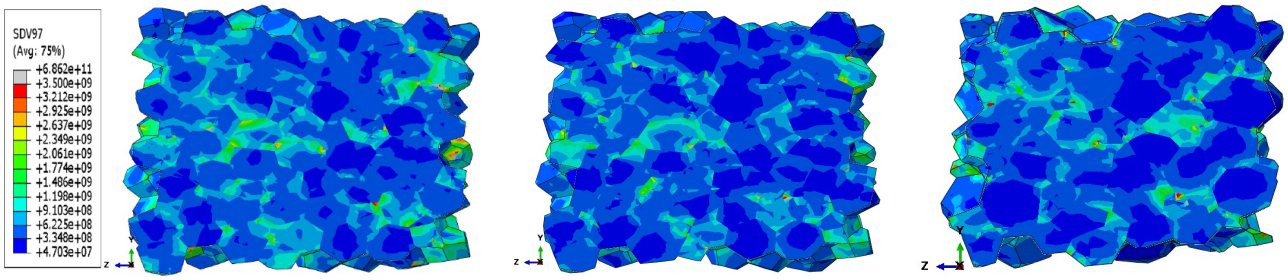

(a) *Uniform grain size GND distribution* (b) *GND distribution for c.o.v=0.1* (c) *GND distribution for c.o.v=0.3*

Fig. 5: *Effect of grain size distribution on GND density: spatial distribution of geometrically necessary dislocation (GND) densities obtained from GECP simulations for an irregular RVE with increasing size distribution. (a) Uniform grain size, evenly spread distribution of regions with higher GND densities (b) c.o.v=0.1, GND distribution spread similar to the uniform case, with less strong localizations (c) c.o.v=0.3, dominant large grain behavior, with a reduction in overall GND accumulation through larger regions with lower GND densities and more localized regions of high density near smaller and highly misoriented grains. Less overall GNDs leads to a reduction in the hardening response*

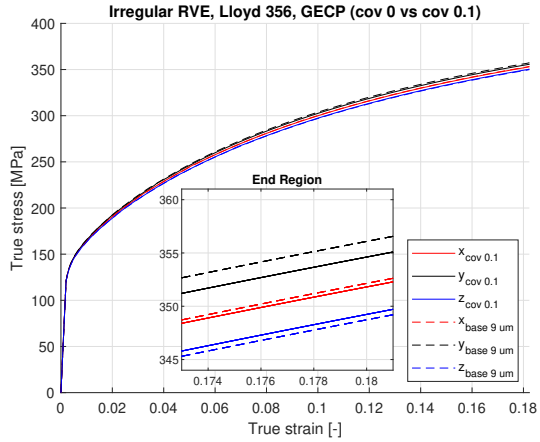

(a) *True stress-strain curves comparison: no size distribution and small grain size variation*

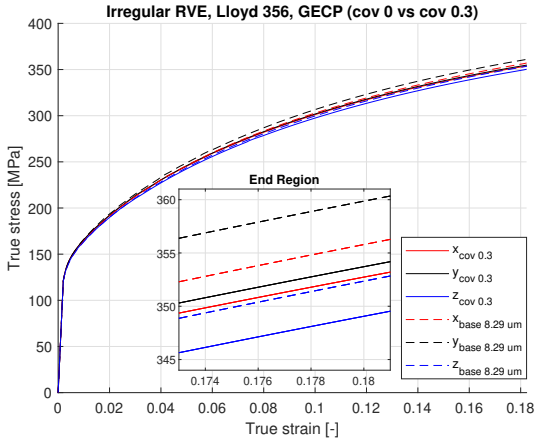

(b) *True stress-strain curves comparison: no size distribution and large grain size variation*

Fig. 6: *GECP simulations true stress-strain results for an irregular RVE with increasing levels of grain size distribution variation. The plots display a comparison of the stress-strain curves between RVEs with uniform grains and RVEs with grains size distribution. (a) Uniform grain morphology (- -) and c.o.v=0.1 (–) (b) uniform grain morphology (- -) and c.o.v=0.3 (–)*

CP and GECP frameworks exhibit nearly identical behavior, with deviations from the uniform grain size simulation stress results below a mean relative error of 0.3%. Grain size distribution does not significantly affect the isotropy of the RVE.

As the grain size distribution becomes broader (c.o.v of 0.3), so called dominant large grain behavior emerges, resulting in a reduction of the hardening percentage, as visible in the stress-strain plots of Fig. 6 . The GECP framework predicts a stress decrease of approximately 1% relative to the uniform grain size RVE for highly heterogeneous microstructures. This reduction in hardening is attributed to lower plastic strain gradients around larger grains and only localized regions of high dislocation densities, which reduce the overall accumulation of GNDs and lower the hardening response, as supported by the spatial distribution plot, Fig. 5c.

The CP framework is unable to capture this decrease in hardening, as it lacks the material length scale associated with strain gradient calculation. While CP simulations reflect variations in stress due

to changes in geometry regularity and altered crystallographic misorientation distributions, it does not capture a systematic dependence on grain size variance for the investigated RVEs.

A direct comparison between CP and GECP simulations highlights the conditions under which the GECP formulation outperforms the latter. For RVEs with uniform grain size or low grain size heterogeneity, the predicted responses are similar.

With increasing grain size variance, however, the GECP formulation provides additional predictive capabilities. The inclusion of strain gradient calculations predicts a reduction in hardening associated with dominant large grain behavior and localized regions of high dislocation density due to the size dependent effects. Quantitatively, the difference between the frameworks for a c.o.v of 0.3 is around 1% decrease in stress. These results indicate that while CP is sufficient for modeling relatively homogeneous microstructures, GECP is more accurate for predicting the mechanical response of heterogeneous polycrystals.

Influence of grain shape (aspect ratio)

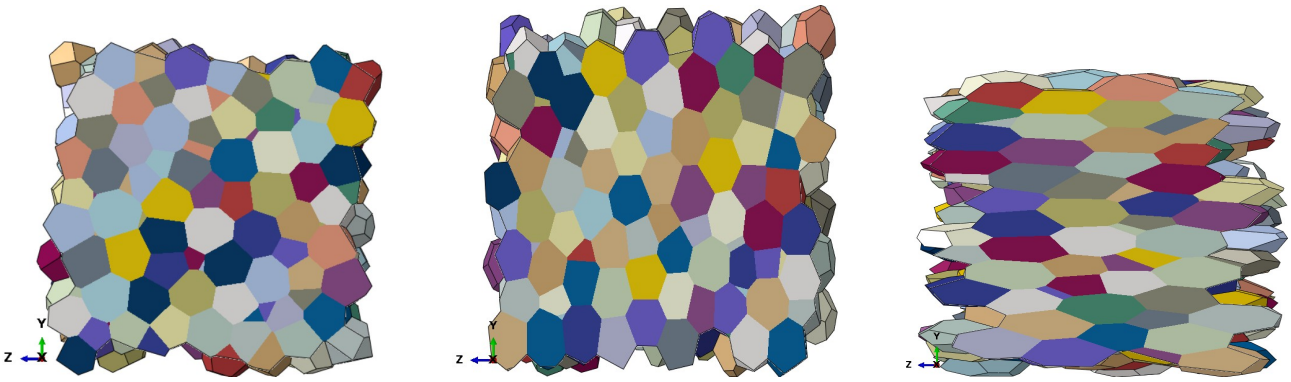

(a) *Uniform grain size* (b) *Aspect ratio 0.75* (c) *Aspect ratio 3*

Fig. 7: *Effect of grain aspect ratio on RVE geometry: Geometry plane cuts (y-z) for 3D periodic irregular RVE with variations in grain aspect ratio along the z axis. (a) Base geometry with uniform grain size, (b) reduced grain aspect ratio of 0.75, compressed grain aspect (c) increased grain aspect ratio of 3, elongated grain aspect*

The influence of grain shape on the macroscopic response is examined by varying the grain aspect ratio while maintaining a fixed average grain size and grain volume fraction. For the investigated RVEs, the grain aspect ratio is varied from 0.75 to 3 along the z-axis, as shown in Fig. 7. The crystallographic lattice orientations are randomly assigned and, where possible, kept identical between RVEs. In the absence of a predominant texture, any anisotropic response observed can be primarily attributed to variations in grain morphology and geometrical arrangement.

For both CP and GECP frameworks, variations in grain aspect ratio lead to small changes in the macroscopic stress-strain response, typically below 1% mean relative error from uniform grain results, Fig. 9. A slight directional dependence is observed, characterized by a reduced resistance to deformation when loading is applied perpendicular to the grain aspect ratio direction. Nevertheless, stress variations across loading directions remain within a narrow range. The inclusion of strain gradient effects in the GECP framework does not predict shape-dependent hardening behavior either, with comparable GND distributions across the investigated RVEs, as shown in Fig. 8.

Overall, for the investigated RVEs, no clear identifiable correlation between grain aspect ratio and macroscopic response or anisotropy is noticed. The observed stress variations are small, remain within numerical tolerance across cases, and are comparable in magnitude to uncertainties arising from geometrical changes. As a result, an exact quantitative assessment for the change in stress solely due to grain shape is hard to attribute. For complete clarity, further studies should be conducted under tight geometrical constraints or through a systematic texture study where unwanted variables are statistically averaged out. The findings indicate that, within the current framework and checked RVEs,

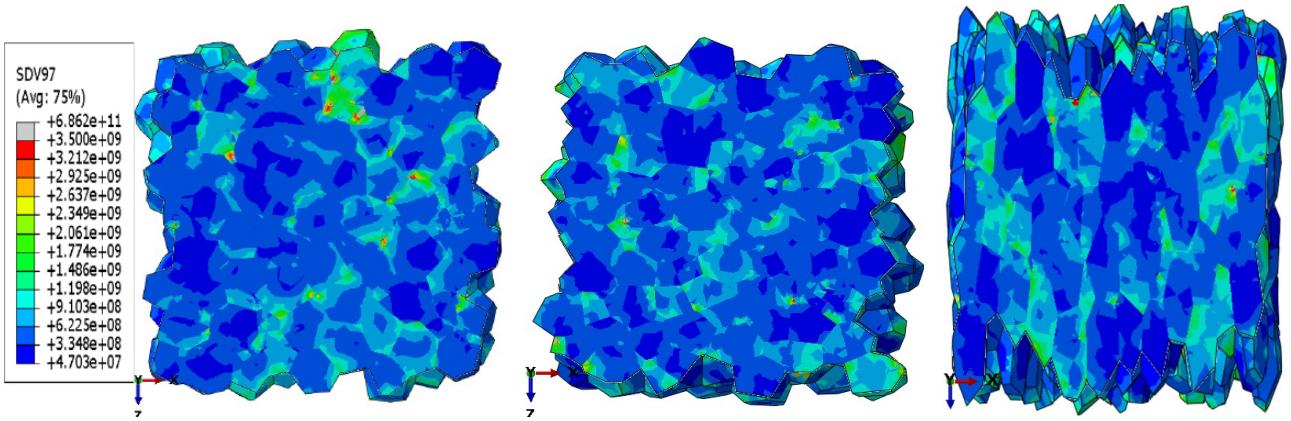

(a) *Uniform grain size GND distribution* (b) *GND distribution for aspect ratio 0.75* (c) *GND distribution for aspect ratio 3*

Fig. 8: *Effect of grain aspect ratio on GND density: spatial distribution of geometrically necessary dislocation (GND) densities obtained from GECP simulations for irregular RVEs with varying aspect ratios, (x-z) plane cut. (a) Uniform grain size, relatively evenly spread distribution regions, (b) aspect ratio 0.75 (c) aspect ratio 3. Comparable GND distributions across all cases, no clear pattern can be distinguished for shape-dependent effects*

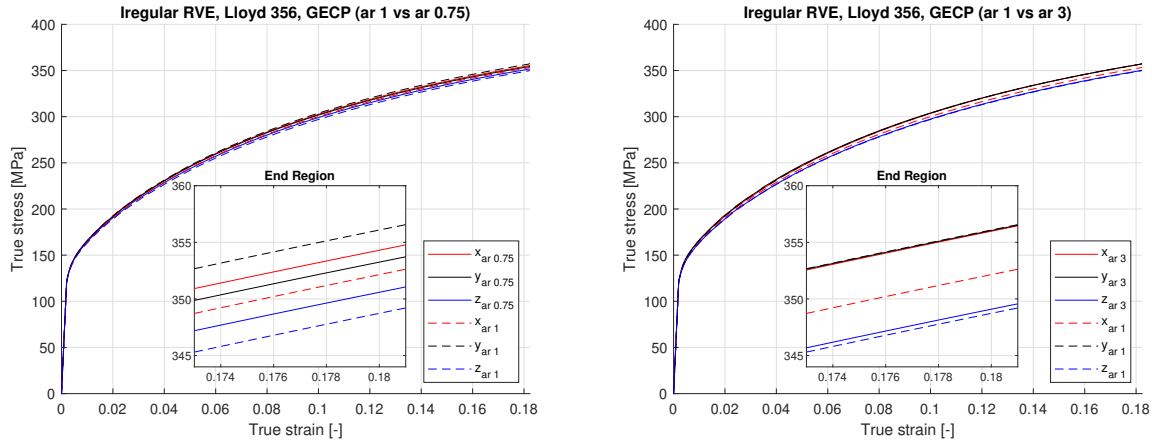

(a) *True stress-strain curves comparison: aspect ratio of 1 and aspect ratio of 0.75* (b) *True stress-strain curves comparison: aspect ratio of 1 and aspect ratio of 3*

Fig. 9: *GECP simulations true stress strain results for an irregular RVE with varying aspect ratios. The plots display a comparison of the stress curves between RVEs with uniform grains and RVEs with grain shape change through aspect ratio assignment. (a) Uniform grain morphology (- -) and aspect ratio 0.75 (–) (b) uniform grain morphology (- -) and aspect ratio 3 (–)*

the influence of grain shape is minor and significantly weaker than that of grain size distribution and crystallographic orientation effects.

Conclusion

The macroscopic response of polycrystalline materials was investigated using three-dimensional representative volume elements within crystal plasticity (CP) and gradient enhanced crystal plasticity (GECP) frameworks. The results show that grain size-dependent work hardening effects are very well represented within GECP formulation through the inclusion of strain gradient calculations and geometrically necessary dislocation evolution. Grain size distribution is further shown to influence the mechanical response of heterogeneous microstructures, with these effects more accurately predicted

by the GECP framework for large variations in grain size. In contrast, no significant variations in the macroscopic response are observed for changes in grain shape in the absence of predominant crystallographic texture for the investigated RVEs. Overall, the findings highlight the capabilities of the frameworks, with the GECP formulation able to provide a more in-depth and reliable representation of heterogeneous polycrystalline materials.

References

[1] R.J.Asaro. Crystal plasticity. *Journal of Applied Mechanics*, 50(4b):921–934, 1983.

[2] J.F.Nye. Some geometrical relations in dislocated crystals. *Acta Metallurgica*, 1(2):153–162, 1953.

[3] A. Acharya and J. L. Bassani. Lattice incompatibility and a gradient theory of crystal plasticity. *Journal of the Mechanics and Physics of Solids*, 48(8):1565–1595, 2000.

[4] N. A. Fleck, M. A. Ashby, and J. W. Hutchinson. The role of geometrically necessary dislocations in giving material strengthening. *Scripta Materialia*, 48(2):179–183, 2003.

[5] E S Perdahcioglu. A rate-independent crystal plasticity algorithm based on the interior point method. *Computer Methods in Applied Mechanics and Engineering*, 418(Part A), 2024.

[6] B Nijhuis, E S Perdahcioglu, and A H van den Boogaard. A robust and efficient rate-independent crystal plasticity model based on successive one-dimensional solution steps. *Computer Methods in Applied Mechanics and Engineering*, 438(Part B), 2025.

[7] Y. Bergstrom. A dislocation model for the stress–strain behaviour of polycrystalline alpha-fe with special emphasis on the variation of the densities of mobile and immobile dislocations. *Materials Science and Engineering*, 5(4):193–200, 1970.

[8] E S Perdahcioglu, C Soyarslan, E E Asik, A H van den Boogaard, and S Bargmann. A class of rate-independent lower-order gradient plasticity theories: Implementation and application to disc torsion problem. *Materials*, 11(8), 2018.

[9] M. F. Ashby. The deformation of plastically non-homogeneous materials. *Philosophical Magazine*, 21(170):399–424, 1970.

[10] L. Kudin, B. Devincre, and M. Tang. Mesoscopic modelling and simulation of plasticity in fcc and bcc crystals: Dislocation intersections and mobility. *Journal of Computer-Aided Materials Design*, 5:31–54, 1998.

[11] M. Becker. *Incompatibility and Instability Based Size Effects in Crystals and Composites at Finite Elastoplastic Strains*. PhD thesis, Institut für Mechanik (Bauwesen), Lehrstuhl I, Universität Stuttgart, 2006.

[12] Lawrence Berkeley National Laboratory. voro++. `https://math.lbl.gov/voro++/about.html`. Accessed 2025-10-15.

[13] C Geuzaine and J-F Remacle. Gmsh: A 3-d finite element mesh generator with built-in pre- and post-processing facilities. *International Journal for Numerical Methods in Engineering*, 79(11):1309–1331, 2009.

[14] R. Bocan. Study on the effects of grain shape, size and size distribution on the mechanical behavior of metals. Master's thesis, University of Twente, 2025.